



저작자표시-비영리-변경금지 2.0 대한민국

이용자는 아래의 조건을 따르는 경우에 한하여 자유롭게

- 이 저작물을 복제, 배포, 전송, 전시, 공연 및 방송할 수 있습니다.

다음과 같은 조건을 따라야 합니다:



저작자표시. 귀하는 원저작자를 표시하여야 합니다.



비영리. 귀하는 이 저작물을 영리 목적으로 이용할 수 없습니다.



변경금지. 귀하는 이 저작물을 개작, 변형 또는 가공할 수 없습니다.

- 귀하는, 이 저작물의 재이용이나 배포의 경우, 이 저작물에 적용된 이용허락조건을 명확하게 나타내어야 합니다.
- 저작권자로부터 별도의 허가를 받으면 이러한 조건들은 적용되지 않습니다.

저작권법에 따른 이용자의 권리는 위의 내용에 의하여 영향을 받지 않습니다.

이것은 [이용허락규약\(Legal Code\)](#)을 이해하기 쉽게 요약한 것입니다.

[Disclaimer](#)

보건학석사 학위논문

**Characteristics of
Free amino acids in PM_{2.5}
measured in Seoul**

서울시 초미세먼지 내 유리 아미노산
농도 특성 파악 연구

2021년 8월

서울대학교 보건대학원
환경보건학과 대기환경전공

이미래

Characteristics of
Free amino acids in PM_{2.5}
measured in Seoul

서울시 초미세먼지 내
유리 아미노산 농도 특성 파악 연구

지도교수 이승묵

이 논문을 보건학석사 학위논문으로 제출함
2021년 5월

서울대학교 대학원
환경보건학과 대기환경전공
이미래

이미래의 보건학 석사 학위논문을 인준함
2021년 7월

위 원 장 _____ 조경덕

부위원장 _____ 김호

위 원 _____ 이승묵

Abstract

Characteristics of Free amino acids in PM_{2.5} measured in Seoul

MiRae Lee

Department of Environmental Health Sciences

The Graduate School of Public Health

Seoul National University

Fine particulate matter (PM_{2.5}) samples collected from December 2019 to November 2020 in Seoul were analyzed for their mass concentration of organic carbon (OC), element carbon (EC), ionic species, trace elements, water-soluble organic carbon (WSOC) and free amino acids (FAAs). WSOC, which is significant portion of OC, showed seasonality in this study. WSOC can be easily absorbed into lung fluids potentially causing adverse health effects. Free Amino acids (FAAs) are ubiquitous proteinaceous compounds in aerosols

and important component of WSOC. Previous study reported that alterations in the amino acids profile in the lung environment due to inhalation of PM_{2.5} may cause the increase in asthmatic inflammation.

In this study, analysis method using HPLC–MS/MS for free amino acid (Aspartic acid, Leucine, Glutamic acid, Phenylalanine, Valine, Serine, Cystine, Methionine, Tyrosine) was developed. However, Cystine and Methionine were not detected in samples during the study period.

The characteristics of free amino acids were discussed with their seasonal variations. Aspartic acid, which was the most dominant FAA species in this study, correlated well with secondary organic carbon (SOC) ($R^2 = 0.64$) and OC ($R^2 = 0.66$) during the warm season (April–September). PSCF results showed that Taiyuan and Shijiazhuang, which are known as main industrial cities in North China, were found to be possible source regions of SOC, Aspartic acid and Glutamic acid. Glutamic acid, Leucine, Tyrosine, Phenylalanine, and Valine showed peak events in May, and the events were presumably influenced by pollen effect. In addition to pollen effect, CPF modeling was performed to estimate the possible source location of Leucine, Tyrosine, Phenylalanine, and Valine. The CPF results showed that high concentration events (upper 25% of each FAA mass concentration) of these compounds were affected by southwest region where the Sihwa–Banwol industrial complex is located. Significant relations between FAAs and ionic species or trace elements in PM_{2.5} were not observed in this study.

From the study results, free amino acids in PM_{2.5} measured in Seoul

may be originated from various sources: (1) SOA due to long-range transport from North China, (2) marine aerosols from Yellow Sea on the Chinese side, (3) the influence of local industry sources and, (4) pollen effect in spring.

Keyword : Fine particulate matter, Water-soluble organic carbon,
Free amino acids, Secondary organic aerosol, HPLC-MS/MS
Student Number : 2019-22005

Table of Contents

Abstract	I
List of Tables.....	VI
List of Figures	VII
Chapter 1. Introduction.....	1
Chapter 2. Sample collection and methods	3
2.1 Sampling	3
2.1.1 Sampling site description.....	3
2.1.2 Sampling method	4
2.2 Analytical methods	6
2.2.1 Ionic species.....	6
2.2.2 Trace elements	6
2.2.3 Organic carbon (OC) and Element carbon (EC) .	7
2.2.4 Water-soluble organic carbon	7
2.2.5 Free amino acids	8
2.2.6 Quality assurance and quality controls.....	9
2.3 EC tracer method	10
2.4 Meteorological parameters and ambient gaseous material data	10
2.5 Statistical methods	11
2.6 Conditional probability function (CPF)	11
2.7 Potential Source Contribution Function (PSCF) ...	1 2
Chapter 3. Results and Discussions.....	13
3.1 Chemical constituents	13
3.2 Characteristics of WSOC and FAAs.....	19
3.2.1 WSOC in PM _{2.5}	19

3.2.2 FAAs in PM _{2.5}	22
Chapter 4. Conclusions	34
Reference.....	36
Supplementary Materials	4 3
국문 초록	5 2

List of Tables

Table 1. The sampling period of this study	5
Table 2. Meteorological parameters during the sampling period	5
Table 3. Summary of PM _{2.5} species concentration during the study period by season.....	16
Table 4. Seasonal differences of WSOC in OC and PM _{2.5}	20
Table 5. Summary of OC, WSOC, and WSOC/OC ratio in previous study	21
Table 6. Summary of each FAA in PM _{2.5} during the study period	27
Table 7. Seasonal differences of total FAA in WSOC, OC ...	29
Table 8. Factor loadings matrix after varimax rotation.	33

List of Figures

Figure 1. Geographical location of sampling site.....	3
Figure 2. Time plots of meteorological parameters and chemical constituents.....	17
Figure 3. Monthly trend of POC and SOC.....	18
Figure 4. Scatter plot of WSOC and SOC (left), WSOC and POC (right).....	20
Figure 5. Time plots of each FAA during the sampling period.....	28
Figure 6. Seasonal differences of FAAs and O ₃ in this study.....	29
Figure 7. Seasonal variations on average mass concentration of FAAs.....	30
Figure 8. Time plots of SOC and Asp.....	30
Figure 9. Scatter plots between SOC and Asp (left) and between OC and Asp (right) in warm season.....	31
Figure 10. PSCF plot of SOC mass concentration.	31
Figure 11. PSCF plot of Asp mass concentration.	32
Figure 12. PSCF result of Glu mass concentration.	32
Figure 13. CPF result of Leu, Phe, Tyr, and Val.....	33

Chapter 1. Introduction

Fine particulate matter ($PM_{2.5}$) is a fine particle with aerodynamic diameter that is less than $2.5 \mu\text{m}$. $PM_{2.5}$ is classified as group 1 carcinogen (WHO, 2013) and it can penetrate deeply into the alveolar region of the lung and cause adverse health effects related to cardiovascular and respiratory diseases (Dominici et al. 2006).

$PM_{2.5}$ is composed of water-soluble ions, heavy metals, organic carbon (OC) and elemental carbon (EC). OC is classified into water-soluble organic carbon (WSOC) and water-insoluble organic carbon (WISOC). WSOC, accounting for 10–80% of OC, is often considered as secondary organic aerosol (SOA) and can alter hygroscopic properties, surface tension and density of aerosols. WSOC includes various species of amines, organic acids and amino acids.

Amino acids (AAs) are ubiquitous proteinaceous compounds in aerosols and important component of WSOC. Although little is known about the major constituents of organic compounds including nitrogen, recent studies suggest that 20–80% of total nitrogen is bound in organic compounds (Zhang et al., 2002; Mace et al., 2003). AAs in atmosphere are separated into combined amino acids (CAAs) and free amino acids (FAAs). Total amino acids (TAAs) is the sum of CAAs and FAAs. AAs affect the atmospheric water cycle because these compounds can be an important source of fixed nitrogen in the environment (Peters and Bruckner-Schatt, 1995). They have effect on the acid-neutralizing capacity of particles because they have basic nitrogen functional groups (Zhang et al., 2002). Since

proteinaceous compounds in aerosols are strong allergens, they can cause respiratory and inflammatory diseases (Di Filippo et al., 2014). Alterations in the amino acids profile in the lung environment due to inhalation of $PM_{2.5}$ may cause the increase in asthmatic inflammation (Peterson et al., 1998). Despite their importance and ubiquity, the fate of AAs in atmosphere and the health effects of inhaling the AAs of $PM_{2.5}$ are poorly understood.

The identification and quantification of AAs in aerosols are difficult because these compounds have high polarity, low volatility, and the lack of strong chromophore groups. They were generally analyzed by HPLC with a fluorescence detector, after derivatization of compounds with o-phthalaldehyde/mercaptoethanol (OPA). However, the drawbacks of using derivatization are (1) time consuming due to preparation for derivatization process, and (2) long retention time on chromatographic separation of some amino acid derivatives (Matos et al., 2016). Recently, studies on method for AAs analysis using liquid chromatography–tandem mass spectrometry (LC–MS/MS) have been reported. Those methods allow the better detection of the trace amounts of AAs in aerosols.

The objectives of this study are (1) to develop LC–MS/MS method for quantification of FAAs in $PM_{2.5}$, (2) to evaluate the seasonal variations of FAAs in $PM_{2.5}$ measured from December 2019 to November 2020 in Seoul, (3) to investigate the potential sources of FAAs in $PM_{2.5}$ measured in Seoul. This is the first study for characterization of FAAs in $PM_{2.5}$ measured in Seoul.

Chapter 2. Sample collection and methods

2.1 Sampling

2.1.1 Sampling site description

In this study, ambient PM_{2.5} samples were collected on the rooftop of Graduate School of Public Health Building at Seoul National University (37.581° N, 127.001° E, 21m above ground level), Which is located on Gwanak Mountain (Figure 1). The regional characteristics of the sampling site are quite complicated, because residential and commercial districts are located near the sampling site. The site is also influenced by industrial complex located in the southwest side of the site. Hence the site is affected by several types of pollutant emissions, such as biogenic, residential, traffic, and industrial emissions.

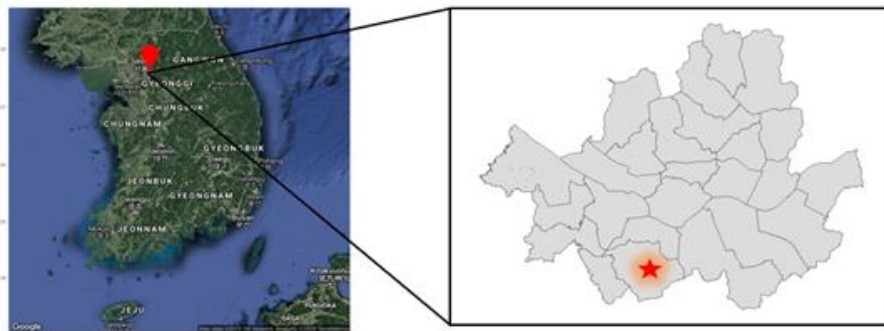


Figure 1. Geographical location of sampling site.

2.1.2 Sampling method

Ambient PM_{2.5} samples (n=71) were collected for 23 hours from December 2019 to November 2020 through 3 channels of low-volume air samplers which are connected with size-selective cyclone (URG-2000-30EH, URG), respectively and the samples with flow rate within the 5% of 16.7 L min⁻¹ were used for analysis processes. Detailed sampling dates are shown in Table 1 and meteorological parameters during the sampling period of this study (temperature and relative humidity) are given in Table 2. Teflon filters (47 mm, 1.0 μm pore size, Pall corporations, USA) for PM_{2.5} mass concentration and trace elements, quartz filters (47 mm, 1.0 μm pore size, Pall corporation, USA) for organic carbon (OC) and element carbon (EC), and PTFE filter (47 mm, 1.0 μm pore size, Pall corporation, USA) for ion species were used with low volume air samplers.

To analyze the WSOC and FAAs in PM_{2.5} which were collected on quartz filter (WhatmanTM, QMA 1851-865, UK), the high-volume air sampler (TE-HVPLUS, TISCH, USA) with flow rate of 40 CFM (cubic feet per minute) was used.

Teflon filter was stored in desiccator for 24 hours before weighing and then was weighed for calculating PM_{2.5} mass concentration using microbalance (Satorius, CP2225D, sensitivity of ± 0.01 mg) before and after sampling. Quartz filters were baked at 450 °C for 12 hours to eliminate pre-existing organic compounds. PTFE filter were soaked with ethanol and distilled deionized water (DDW, 18.2 MΩ cm

of conductivity). All collected samples were kept in the freezer until chemical analysis.

Table 1. The sampling period of this study

Season	Month	Sampling date
winter (n=18)	December – February	2019. 12 – 2020. 02
spring (n=18)	March – May	2020. 03 – 2020. 05
summer (n=17)	June – August	2020. 06 – 2020. 08
fall (n=18)	September – November	2020. 09 – 2020. 11

Table 2. Meteorological parameters during the sampling period

Season	Temperature (°C)	Relative Humidity (%)
winter	-2.25 ± 3.68	77.7 ± 12.3
spring	8.73 ± 4.02	61.8 ± 21.9
summer	20.9 ± 2.11	83.9 ± 15.7
fall	11.0 ± 6.37	73.9 ± 13.7

2.2 Analytical methods

2.2.1 Ionic species

Ionic species are classified into anion and cation. Anion (NO_3^- , SO_4^{2-} , Cl^-) and cation (NH_4^+ , K^+) were analyzed using Ion chromatography (IC, Dionex CO., DX-1100, USA). PTFE filter after sampling were extracted in 30 mL of DDW (Deionized Distilled Water) for 4 hours, 40°C using ultrasonic extraction method. The extract was filtered through a 0.22 μm syringe filter (PALL science, 0.22 μm pore size) and then analyzed by IC. The anion column (Ionpac AS14A 4, 250 mm) and the cation column (Ionpac CS12A 4, 250 mm) were used for IC analysis. Blank values were subtracted to calculate ionic species concentration.

2.2.2 Trace elements

The trace elements in $\text{PM}_{2.5}$ collected on the teflon filter were analyzed by non-destructive energy dispersive X-Ray fluorescence (XRF) spectrometer. The target trace elements for XRF analysis are approximately 20 species (Al, Si, Mg, Cl, Ca, Cr, Fe, K, Mn, Pb, Ti, V, Zn, Ni, As, S, Se, Ba, Br, etc.).

2.2.3 Organic carbon (OC) and Element carbon (EC)

The carbon Aerosol analyzer (Model 3, Sunset Laboratory Inc., USA) was performed to analyze the concentration of OC and EC in PM_{2.5}. The quartz filter was punched to 1.5 cm² and analyzed using the thermal/optical transmittance (TOT) method with the National Institute of Occupational Safety and Health (NIOSH) 5040 protocol (Table S1).

2.2.4 Water-soluble organic carbon

Quartz filter collected PM_{2.5} by high-volume air sampler was ultrasonically extracted in two steps, with 20 mL and 10 mL of DDW. The extracts were combined, and filtered through a 0.22 μm syringe filter (PALL science, 0.22 μm pore size) and analyzed by TOC analyzer (TOC 5000, Shimadzu, Japan). The total carbon (TC) standard was made using potassium hydrogen phthalate (Sigma-Aldrich, St.Louis, USA) and inorganic carbon (IC) standard was made using sodium carbonate (Sigma-Aldrich, St.Louis, USA) and sodium bicarbonate (Sigma-Aldrich, St.Louis, USA). The calibration was performed by using the 'TC-IC' method.

2.2.5 Free amino acids

Quartz filter collected PM_{2.5} by high-volume air sampler was ultrasonically extracted with 10 mL of DDW for 30 min. The extract was filtered through a 0.22 μm syringe filter (PALL science, 0.22 μm pore size) and analyzed by High performance liquid chromatography-tandem mass spectrometry (UHPLC Nexera, Shimadzu, Japan; API 4000, SCIEX, Canada) with poroshell C18 column (2.1 \times 150 mm, 4.0 μm , Agilent, USA). The high standard stock solution was prepared by dissolving L-aspartic acid, L-cystine, L-glutamic acid, L-leucine, L-methionine, L-phenylalanine, L-serine, L-tyrosine, and L-valine to 0.1N hydrochloric acid (HCl), respectively and eluted using 0.1% formic acid in DDW. DL-phenylalanine- β,β -d₂ (d₂-phe) was used as an internal standard. These compounds were purchased from Sigma-Aldrich (St.Louis, USA). The column was heated to 40°C and the sample injection volume and flow rate were 10 μL and 0.25 mL min⁻¹, respectively. Electrospray ionization (ESI) was used in positive mode. Multiple reaction monitoring (MRM) mode was used for free amino acid detection (Table S3) and the parameters (Table S2) for the MRM transitions were as follows: collision gas (CAD) of 7 (arbitrary units), curtain gas (CUR) of 20 (arbitrary units), ion source gas 1 and 2 pressure of 45 and 50 (arbitrary units), respectively. Ionspray voltage of 3500 V, source temperature at 300 °C. For elution of the amino acids 0.1% formic acid in DDW (eluent A) and 0.1% formic acid in acetonitrile (eluent B) were applied. The LC gradient steps were

programmed as follows: at the beginning, 5% eluent B was used for 2 min. eluent B reached 10% at 3 min and 100% at 4 min and kept during 2 min to wash the column. To equilibrate the column, the total run time was 10 min (Table S4).

2.2.6 Quality assurance and quality controls (QA/QC)

The quality assurance and quality control (QA/QC) of free amino acids analysis was performed in this study. Calibration curves of FAAs were used with 6 points of standards (Table S6, FigureS3). The coefficient of determination of individual FAA calibration curve was 0.996–1.000. The limit of detection (LOD) and the limit of quantification (LOQ) were determined by evaluating the signal to noise ratio of three and ten times respectively (Table S5). The concentration results below the LOD were assigned as ‘Not detected (N.D.)’.

To evaluate the recovery, five spiked cleaned quartz filters were extracted in the same manner as samples. The recovery range (70–114%) and relative standard deviations (RSD, 0.86–6.3%) were acceptable (Table S6).

2.3 EC tracer method

The EC tracer method, which was suggested by Turpin and Huntzicker (Turpin and Huntzicker et al., 1995), was used to estimate the POC and SOC. SOC is calculated by using Equation (1).

$$\text{Equation (1) } \text{SOC} = \text{OC} - ([\text{OC}/\text{EC}]_{\text{pri}} \times \text{EC}) - \text{OC}_{\text{non-comb}}$$

POC consists of OC_{comb} which is emitted directly from a combustion source and $\text{OC}_{\text{non-comb}}$ from primary non-combustion emissions such as biogenic sources (Kim et al., 2020). In this study, the slope and y-intercept were used as the $[\text{OC}/\text{EC}]_{\text{pri}}$ ratio and $\text{OC}_{\text{non-comb}}$, respectively.

2.4 Meteorological parameters and ambient gaseous material data

Hourly meteorological data (temperature, relative humidity, etc.) during the sampling period were obtained from Korea meteorological agency (<https://data.kma.go.kr>). Hourly ambient ozone (O_3) data closest to the $\text{PM}_{2.5}$ sampling site were obtained from Air Korea (<http://www.airkorea.or.kr/realSearch>).

2.5 Statistical methods

Factor analysis (FA) were performed using SPSS 22.0 software (SPSS Inc., USA). In FA, the factors with eigenvalues greater than 1 were considered and the varimax rotation was used for rotation.

2.6 Conditional probability function (CPF)

CPF model calculates the probability that a source is located within a particular direction of wind. High CPF value means that the sources are likely to be located on the directions. CPF is calculated by using Equation (2).

$$CPF = \frac{m_{\Delta\theta}}{n_{\Delta\theta}}$$

where $n_{\Delta\theta}$ is the total number of data from $\Delta\theta$, $m_{\Delta\theta}$ is the total number of occurrences from wind sector $\Delta\theta$ that exceed the given value (Choi et al., 2013). In this study, the upper 25th percentile concentration of chemical species in $PM_{2.5}$ was used as the given value.

2.7 Potential Source Contribution Function (PSCF)

PSCF value is the conditional probability that an air parcel that passed through the (i,j)th cell had a high concentration of a pollutant upon arrival at the sampling site. PSCF model is used to identify the likely location of the regional sources for long-range transport aerosols (Choi et al., 2013). PSCF value is calculated by using Equation (3).

$$PSCF = \frac{m_{ij}}{n_{ij}}$$

Where n_{ij} is the total number of end points that fall in the (i,j)th cell and m_{ij} is the number of end points in the same cell associated with samples that exceed the threshold concentration level. In this study, the criteria value of m_{ij} was assigned to upper 25% mass concentration of chemical species in $PM_{2.5}$. High PSCF value means that the potential source areas are likely to be located in the area. PSCF is a hybrid model which combines chemical speciation data and backward trajectory of receptor sites which are obtained from NOAA HYSPLIT 4 model using Global Data Assimilation System 1.0 (GDAS 1.0: data resolution of $1.0^\circ \times 1.0^\circ$). Three-day (72 hours) backward trajectories for every three hours were analyzed to identify the air parcels arriving at the sampling site. The starting height of backward trajectory was set to half of the Planetary Boundary Layer (PBL).

Chapter 3. Results and Discussions

3.1 Chemical constituents

In this study, PM_{2.5} samples (n=71) over a year were selected for chemical analysis considering ion balance (within 0.5–1.5). Of the 9 species of FAAs, 6 species (Asp, Leu, Phe, Tyr, Val, and Glu) were identified and quantified (Table 3). Although Ser was detected in PM_{2.5} samples, it was excluded because the relative standard deviation (RSD) of the samples exceeded 20%.

The mass concentration of chemical species in PM_{2.5} are summarized as a geometric mean (Table 3) because the data are right-skewed. Time series plots of PM_{2.5} speciation data of the study period are shown in Figure 2. The average PM_{2.5} mass concentration during the this study period was $24.4 \pm 1.78 \mu\text{g}/\text{m}^3$, which exceeded the annual PM_{2.5} standards ($15 \mu\text{g}/\text{m}^3$) in Korea and US EPA (2012). In winter ($33.1 \pm 1.88 \mu\text{g}/\text{m}^3$) and spring ($28.7 \pm 1.66 \mu\text{g}/\text{m}^3$) of this study period, the PM_{2.5} mass concentration were higher than summer ($17.8 \pm 1.50 \mu\text{g}/\text{m}^3$) and fall ($20.5 \pm 1.74 \mu\text{g}/\text{m}^3$). The annual average concentration of OC and EC were $4.51 \pm 1.58 \mu\text{g}/\text{m}^3$ and $0.32 \pm 1.53 \mu\text{g}/\text{m}^3$, respectively. OC can be emitted into atmosphere as POC (primary organic carbon) or SOC (secondary organic carbon). POC is directly emitted into atmosphere whereas SOC is generated secondarily through a gas-to-particle conversion process. When divided into cold (Dec 2019, Jan – Feb, Sep – Dec

2020, average temperature: 2.4 °C) and warm seasons (Apr – Sep 2020, average temperature: 16.7 °C), OC concentration during the cold season was relatively dominated by POC due to influence of district heating. Since Heavy rainfall (the average: 45 mm) event occurred in August, SOC is decreased because of the solar radiation reduction due to rainfall that can slow down the atmospheric oxidation (John and Spyros, 2006). The annual average concentration of WSOC was $1.90 \pm 1.81 \mu\text{g}/\text{m}^3$. The highest seasonal concentration of WSOC was in Spring ($2.50 \pm 1.63 \mu\text{g}/\text{m}^3$) and it is followed by winter ($2.20 \pm 1.44 \mu\text{g}/\text{m}^3$). Since ozone level increased in spring and summer as shown in Figure 2, WSOC/OC ratio in spring (0.51) and summer (0.51), which were relatively higher than fall (0.31) and winter (0.37), reflected the enhancement of secondary organic aerosol (SOA) formation.

The annual average concentration of ionic species (NO_3^- , SO_4^{2-} , and NH_4^+) were $3.89 \pm 3.73 \mu\text{g}/\text{m}^3$, $3.96 \pm 1.86 \mu\text{g}/\text{m}^3$, and $2.92 \pm 2.16 \mu\text{g}/\text{m}^3$, respectively. The trace elements in $\text{PM}_{2.5}$ can be classified into crustal elements and non-crustal elements. A concentration of crustal elements was calculated by using Equation (4). The non-crustal elements, which are considered as anthropogenic compounds, consist of these compounds: Mg, Cl, V, Cr, Ni, Cu, Zn, As, Se, and Pb. The annual average concentration of crustal elements and non-crustal elements were $1.62 \pm 1.82 \mu\text{g}/\text{m}^3$ and $0.33 \pm 2.53 \mu\text{g}/\text{m}^3$, respectively.

Equation (4): $\Sigma\text{Crustal elements} = 1.889[\text{Al}] + 2.139[\text{Si}] +$

$$1.205[\text{K}] + 1.4 [\text{Ca}] + 1.668 [\text{Ti}] + 1.43 [\text{Fe}]$$

The total FAAs in $\text{PM}_{2.5}$ is a sum of Asp, Leu, Phe, Tyr, Val, and Glu and the annual average concentration was $107 \pm 2.81 \text{ ng/m}^3$. More details about WSOC and FAAs are discussed in ‘Characteristics of WSOC and FAAs’ in this study.

Table 3. Summary of PM_{2.5} species concentration during the study period by season (geometric mean±geometric standard deviation)

Season	Annual	Winter (Dec 19– Feb 20)	Spring (Mar– May 20)	Summer (Jun–Aug 20)	Fall (Sep – Nov 20)
Species	n = 71	n = 18	n = 18	n = 17	n = 18
PM _{2.5} ($\mu\text{g}/\text{m}^3$)	24.4±1.78	33.1±1.88	28.7±1.66	17.8±1.50	20.5±1.74
OC ($\mu\text{g}/\text{m}^3$)	4.51±1.58	5.45±1.49	4.90±1.43	3.16±1.67	4.82±1.48
EC ($\mu\text{g}/\text{m}^3$)	0.32±1.53	0.38±1.43	0.30±0.40	0.23±1.36	0.39±1.61
POC ($\mu\text{g}/\text{m}^3$)	2.29±1.53	2.72±1.43	2.16±1.40	1.63±1.36	2.79±1.60
SOC ($\mu\text{g}/\text{m}^3$)	1.96±2.29	2.22±2.69	2.60±1.64	1.38±2.28	1.80±2.38
WSOC ($\mu\text{g}/\text{m}^3$)	1.90±1.81	2.20±1.44	2.50±1.63	1.60±1.97	1.48±1.91
NO ₃ ⁻ ($\mu\text{g}/\text{m}^3$)	3.89±3.73	8.97±2.43	6.88±2.26	0.93±3.06	3.71±3.19
SO ₄ ⁻ ($\mu\text{g}/\text{m}^3$)	3.96±1.86	4.74±1.92	3.57±1.77	4.84±1.71	3.04±1.88
NH ₄ ⁺ ($\mu\text{g}/\text{m}^3$)	2.92±2.16	4.21±2.14	3.54±1.81	2.27±1.64	2.11±2.60
Σ crustal elements ($\mu\text{g}/\text{m}^3$)	1.62±1.82	1.73±1.58	1.77±1.45	1.31±2.30	1.68±1.91
Σ non -crustal element ($\mu\text{g}/\text{m}^3$)	0.33±2.53	0.73±1.70	0.43±1.81	0.12±2.13	0.31±2.26
FAAs (ng/m ³)					
Asp	76.8±2.67	27.2±1.89	101±2.39	88.7±2.47	138±1.96
Leu	4.95±2.57	2.42±1.48	6.98±2.83	2.54±1.65	6.01±2.39
Phe	5.68±1.75	N.D.	8.16±2.30	4.42±1.19	5.41±1.47
Tyr	58.2±2.26	N.D.	58.2±2.26	N.D.	N.D.
Val	8.27±2.48	4.15±1.34	15.7±2.77	5.26±1.81	6.22±1.68
Glu	20.0±3.17	6.87±1.76	47.7±3.31	14.9±2.99	21.1±2.01
Total FAAs	107±2.81	38.2±1.74	180±2.70	119±2.33	201±1.51

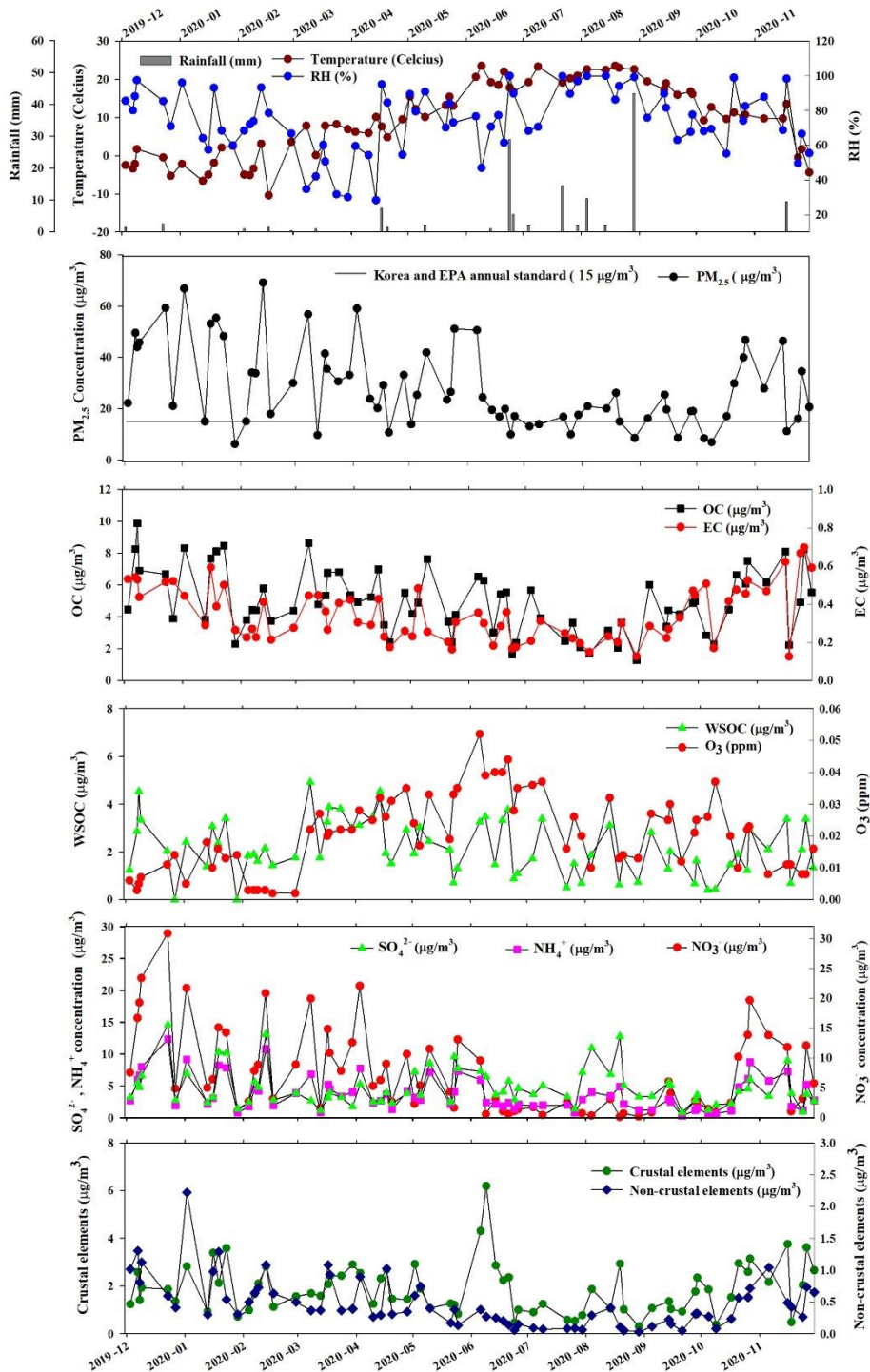


Figure 2. Time plots of meteorological parameters and chemical constituents in $PM_{2.5}$ during the sampling period.

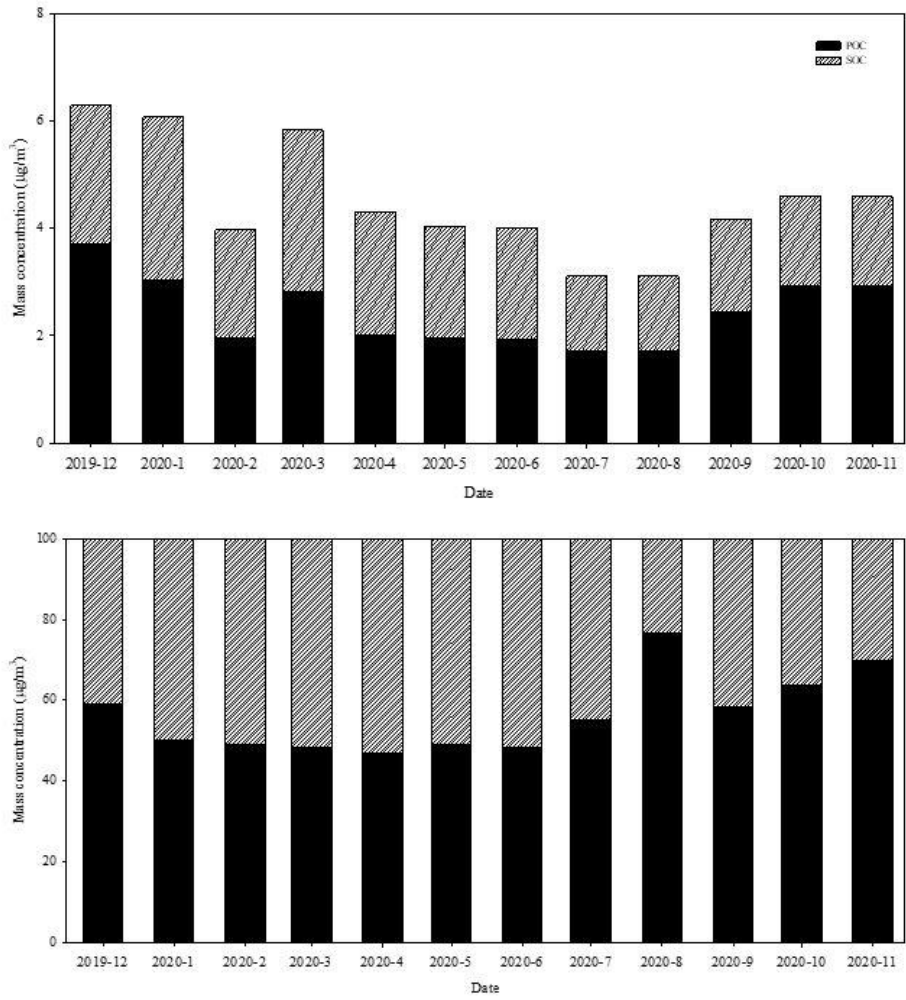


Figure 3. Monthly trend of POC and SOC.

3.2 Characteristics of WSOC and FAAs

3.2.1 WSOC in PM_{2.5}

The concentration of WSOC contributed 42% of OC and 7.6% of PM_{2.5} annually in Seoul. WSOC/OC ratio is used as an indicator of SOA formation due to their polar character and preferentially soluble in water (Kondo et al., 2007). WSOC/OC ratio can be also used to estimate the formation of water-soluble secondary organic aerosol via gas-to-particle conversion during long-range transport (Aggarwal et al., 2010).

The relatively high WSOC/OC ratio during the spring (0.29–0.66) and summer (0.21–0.86) compared with those obtained in winter (0.00–0.48) and fall (0.14–0.47). WSOC/OC ratio in warm season (0.51) was higher than cold season (0.36) significantly (Mann-Whitney Rank sum test, $p < 0.005$). The concentration of WSOC measured in this study were lower than that of Daejeon and Gwangju study (Table 5). But the seasonal trend of WSOC/OC ratio is similar with previous studies.

As shown in Figure 4, WSOC was correlated well with SOC ($R^2 = 0.60$), compared to POC ($R^2 = 0.16$). Thus, significant portion of OC may be more photo-chemically oxidized in the form of WSOC in the warm season than in the cold season.

Table 4. Seasonal differences of WSOC in OC and PM_{2.5}

Fraction	WSOC/OC	WSOC/PM _{2.5}
Annual	0.415	0.076
Winter	0.374	0.058
Spring	0.511	0.087
Summer	0.508	0.090
Fall	0.306	0.072

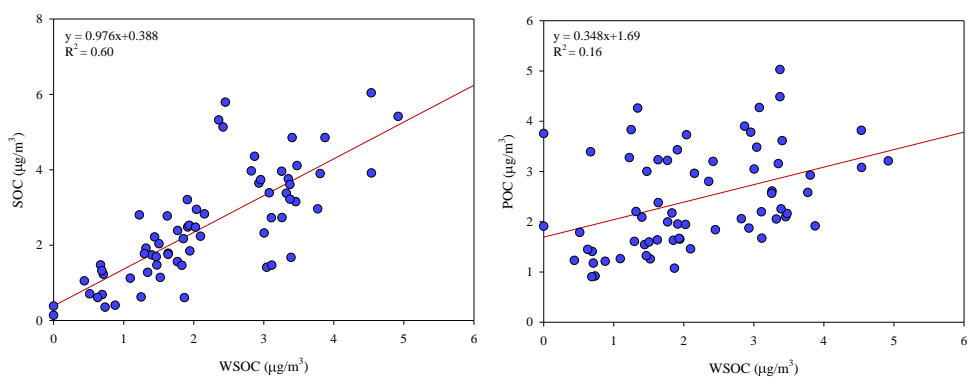


Figure 4. Scatter plot of WSOC and SOC (left), WSOC and POC (right).

Table 5. Summary of OC, WSOC, and WSOC/OC ratio in previous study

Sampling site	Aerosol Type	Season	PM _{2.5}	OC	WSOC	WSOC/OC	Reference
Gosan, Jeju (background site)	PM _{2.5}	Spring	–	4.19	1.26	0.30	Sahu et al., 2009
Gwangju, Korea (urban)	PM _{2.5}	Summer	25.1	5.01	2.77	0.55	Park et al., 2001
		Winter	37.2	8.35	3.66	0.43	
Seoul, Korea (urban)	PM ₁₀	Spring	102	6.53	1.82	0.50	Lee et al., 2011
		Summer	30.1	5.27	2.65	0.46	
		Fall	53.3	9.00	2.89	0.34	
		Winter	75.6	14.3 0	6.65	0.47	
Daejeon, Korea (urban)	PM _{2.5}	Spring	28.7	5.77	3.37	0.58	Kim et al., 2015
		Summer	13.7	3.07	1.77	0.58	
		Fall	22.6	5.84	3.23	0.55	
		Winter	29.5	6.57	4.07	0.62	
Nanjing (urban)	PM _{2.5}	Winter	–	15.6 0	4.70	0.30	Ho et al., 2007
Beijing (urban)	PM _{2.5}	Summer	–	–	3.40	0.39	Cheng et al., 2001
		Winter	–	–	7.30	0.22	

3.2.2 FAAs in PM_{2.5}

The concentration of total FAAs contributed 5.1% of WSOC, 2.2% of OC annually. As shown in Table 6, The concentration of total FAAs was ranged from ‘N.D.’ to $0.962 \mu\text{g}/\text{m}^3$ with an average of $0.107 \pm 2.81 \mu\text{g}/\text{m}^3$ annually. In general, all FAAs showed the lowest concentration in winter. The average concentration of total FAAs was the highest in spring ($0.180 \pm 2.70 \mu\text{g}/\text{m}^3$), which was over 5 times higher than that of winter ($0.035 \pm 1.78 \mu\text{g}/\text{m}^3$). Among the investigated FAAs in this study, Asp was the most dominant species, contributing 66% of total FAAs annually. Subsequently, Glu (21%), Val (4.2%), Leu (3.6%), Phe (2.9%), and Tyr (1.8%) accounted for the total FAAs annually.

Asp was detected in samples regardless of the season or month. During the warm season, Asp was not only correlated well with SOC ($R^2=0.64$) but also with OC ($R^2=0.66$) during the warm season (Figure 9), whereas correlations between Asp and POC ($R^2=0.24$) or EC ($R^2=0.27$) were much weaker (Figure S4). The formation of FAAs in aged aerosols by atmospheric chemical reactions such as direct photolysis, photocatalytic hydrolysis and, enzyme-based hydrolysis of CAAs, has been suggested in previous studies (Milne and Zika, 1993; McGregor and Anatasio, 2001). Asp can be produced via hydroxyl radical attack of asparagine (Milne and Zika, 1993). Hydroxyl radicals are produced by the photolysis of nitrous acid (HONO) in polluted atmosphere. The ozone formation via photolysis of nitrogen dioxide (NO_2) and the fast reaction of electronically

excited NO_2 and water vapor can indirectly produce the hydroxyl radicals in atmosphere (Villena et al., 2011). Since ozone level increased in spring and summer as shown in Figure 6, the observation can be interpreted as the aerosol aging–photochemical transformation. Although the definitive atmospheric half–life of Asp has not been reported, the reaction rate constants of Asp with atmospheric oxidants such as hydroxyl radical similar to those of Glycine and Alanine, which are known as unreactive FAAs, have been reported (Milne and Zika, 1993). Therefore, it can be assumed that Asp was formed while long–range transport and reached the sampling site.

PSCF results showed that Taiyuan in the Shanxi province and Shijiazhuang in the Hebei province may be the possible source regions that affected high concentration events of SOC and Asp. Taiyuan is important industrial location in Shanxi province, where the main industries are coal mining, stainless steel and aluminum manufacturing and chemical fertilizer manufacturing. Shijiazhuang is main industrial city in North China. Industrial complexes such as pharmaceuticals, chemicals production and automobile manufacturing are located in Shijiazhuang. Hence, the gaseous aliphatic amines, which are strong base and emitted from these industrial activities may undergo rapid acid–base reactions to form salt particles in the presence of atmospheric acids such as HCl , HNO_3 , H_2SO_4 or may also react with atmospheric oxidants such as O_3 and NO_x contributing to SOA formation (Murphy et al., 2007).

Leu, Phe, Tyr, Val, and Glu showed the prominent seasonality with

high values in spring (Figure 5). These FAAs peaked in May and these peak events presumably reflected the airborne pollen effect. For example, Pine pollen, which is known as allergenic pollen, is generally released with large quantities in May (Shin et al., 2020). Considering the characteristics of sampling site located in Gwanak Mt., the peak events are reasonably interpreted as the pollen effect. In addition to the pollen effect that appeared only in May, CPF modeling was applied for high concentration events (upper 25 percentile of each FAA mass concentration) of Leu, Val, and Phe to estimate the possible source location of these compounds (Figure 13). Since Tyr was only detected in May, the criterion value for high concentration was upper 3 percentile of mass concentration to perform the CPF modeling. CPF results suggested that the high concentration events of these compounds were commonly influenced by the southwest region. In this region, Sihwa–Banwol industrial complex is located. The main types of the industrial complex are machinery, electronics, food processing and chemicals manufacturing such as pharmaceutical and fertilizer. Since amino acids are commonly used in fertilizer, feed, and food processing as preservatives, flavor or nutrition enhancers (Size, 2020), these types of industries may be emission sources of FAAs.

For Glu, PSCF modeling (Figure 12) was also performed to confirm the possibility of long–range transport because it has low photochemical reactivity with a half–life longer than 19 days in aqueous phase (McGregor and Anastasio, 2001). The samples of May in this study were excluded for PSCF modeling because they were

affected by pollen effect. As shown in Figure 12, the possible source regions were Taiyuan and Shijiazhuang, the same as SOC and Asp. Additionally, Yellow Sea on the Chinese side may be the possible source region of Glu. The result showed that the emission source of Glu can be a marine origin, such as phytoplankton (Cowie and Hedges, 1992; Matsumoto and Uematsu, 2005).

A factor analysis applying varimax rotation was also performed to confirm the possible relations between each FAA. Tyr was excluded from the factor analysis because this compound was only detected in less than half of the total number of samples. The samples of May in this study, which were affected by pollen effect previously described in this paper, were also excluded. Three factors explained 89% of the cumulative variance. The loadings (values in bold greater than 0.7), as shown in Table 8, were used to find the correlation between variables and factors. The first factor linking the Leu, Phe, Val, and Glu may indicate that these compounds have the same origin. In addition, the concentration of Leu and Phe ($R^2=0.72$, $p<0.0001$), Leu and Val ($R^2=0.77$, $p<0.0001$), Phe and Val ($R^2=0.70$, $p<0.0001$), Phe and Glu ($R^2=0.72$, $p<0.0001$) and Val and Glu ($R^2=0.88$, $p<0.0001$) are highly correlated, suggesting similar emission sources. These compounds have a wide range of reactivities in atmosphere. Glu, which is used by almost all living beings in the biosynthesis of proteins, is regarded as relatively unreactive FAA with a half-life greater than 19 days in aqueous phase as stated above. The wide range of amino acids reactivities in atmosphere can be used to determine atmospheric transport of particles (McGregor and

Anastasio, 2001). Met is rapidly destroyed by O₃ in atmosphere (half-life of 2.5 hour). However, Met was not detected in every sample. Tyr is regarded as a reactive FAA with electron-rich side chains so its instability can be indicator of local source (Milne and Zika 1993). Therefore this factor may also indicate a combination of various biogenic sources (pollen, bacteria, and plants) and anthropogenic sources (food or chemical fertilizer industry as stated in CPF results), or an influence of both long-range and locally-derived aerosols (E.Scalabrin et al., 2012). The second factor links SOC and Asp so this factor represents SOA formation. In final factor, the only variable with value greater than 0.7 was POC. The FA result may indicate that the possible sources of FAAs are quite complicated, i.e., FAAs are not only emitted into atmospheric directly but also produced secondarily in atmosphere.

Significant relations between EC or POC and Each FAA were not observed in this study. The result showed that the contribution of combustion related sources are of minor importance (M.Mandalakis et al, 2011). In a previous study, biomass burning as a source of organic compounds containing nitrogen was identified but a significant relation with elemental carbon or K⁺, commonly used marker of biomass burning, was not observed. Similarly, both ionic and trace elements did not show any significant relation with FAAs.

Table 6. Summary of each FAA in PM_{2.5} during the study period (geometric mean±geometric standard deviation)

FAAs	Annual		Winter (n=18)		Spring (n=18)		Summer (n=17)		Fall (n=18)	
	Range	Mean±SD	Range	Mean±SD	Range	Mean±SD	Range	Mean±SD	Range	Mean±SD
Asp ($\mu\text{g}/\text{m}^3$)	N.D.-0.338	0.076±2.67	N.D.-0.069	0.027±1.89	N.D.-0.295	0.101±2.39	0.016-0.317	0.089±2.47	0.018-0.338	0.138±1.97
Leu ($\mu\text{g}/\text{m}^3$)	N.D.-0.072	0.005±2.55	N.D.-0.003	0.002±1.48	N.D.-0.072	0.070±2.83	N.D.-0.005	0.003±1.65	N.D.-0.062	0.006±2.39
Phe ($\mu\text{g}/\text{m}^3$)	N.D.-0.058	0.006±1.75	N.D.	N.D.	N.D.-0.057	0.008±2.30	0.003-0.006	0.004±1.19	N.D.-0.020	0.005±1.47
Tyr ($\mu\text{g}/\text{m}^3$)	N.D.-0.127	0.058±2.26	N.D.	N.D.	N.D.-0.127	0.058±2.26	N.D.	N.D.	N.D.	N.D.
Val ($\mu\text{g}/\text{m}^3$)	N.D.-0.081	0.008±2.48	N.D.-0.005	0.004±1.34	N.D.-0.080	0.016±2.77	N.D.-0.009	0.005±1.81	N.D.-0.013	0.006±1.68
Glu ($\mu\text{g}/\text{m}^3$)	N.D.-0.383	0.020±3.17	N.D.-0.014	0.007±1.76	0.003-0.383	0.048±3.31	N.D.-0.051	0.015±2.99	N.D.-0.066	0.021±2.01
Total FAAs ($\mu\text{g}/\text{m}^3$)	N.D.-0.962	0.106±2.81	N.D.-0.076	0.035±1.78	0.024-0.962	0.180±2.70	0.027-0.376	0.111±2.39	0.018-0.402	0.176±2.01

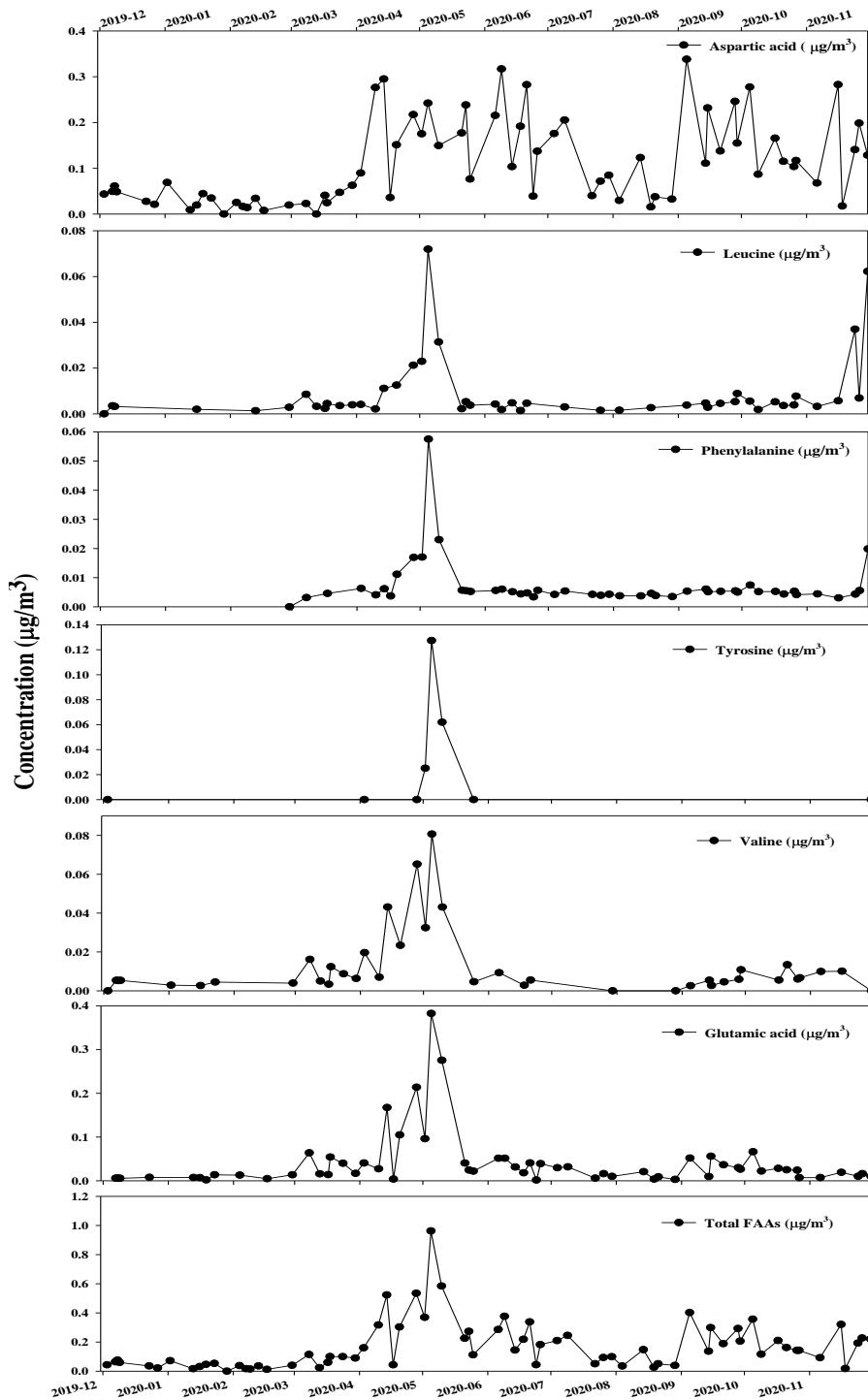


Figure 5. Time plots of each FAA during the sampling period.

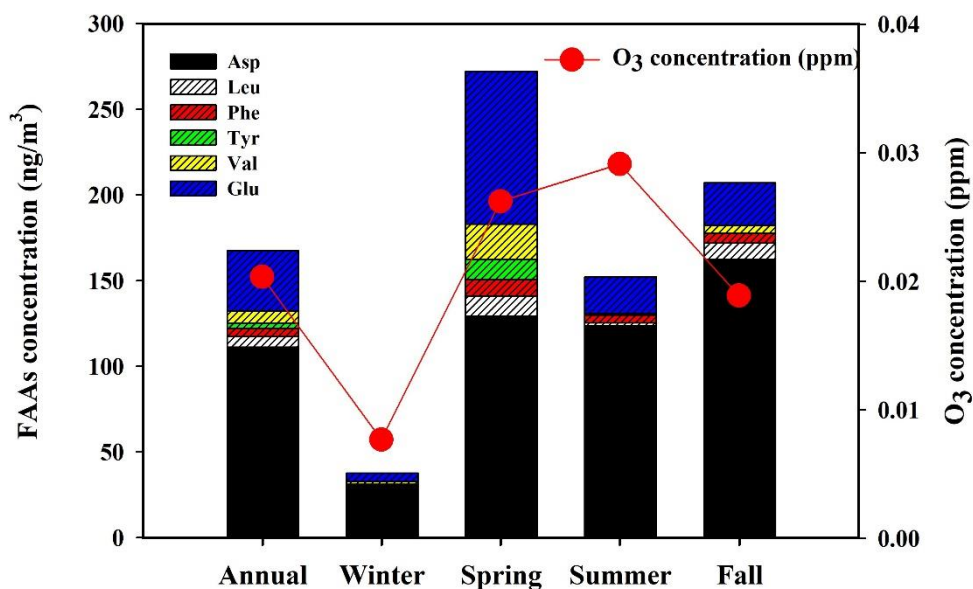


Figure 6. Seasonal differences of FAAs and O₃ in this study.

Table 7. Seasonal differences of total FAA in WSOC, OC, and PM_{2.5}

Fraction	Total FAAs/WSOC	Total FAAs/OC
Annual	0.051	0.022
Winter	0.016	0.006
Spring	0.072	0.037
Summer	0.069	0.035
Fall	0.083	0.029

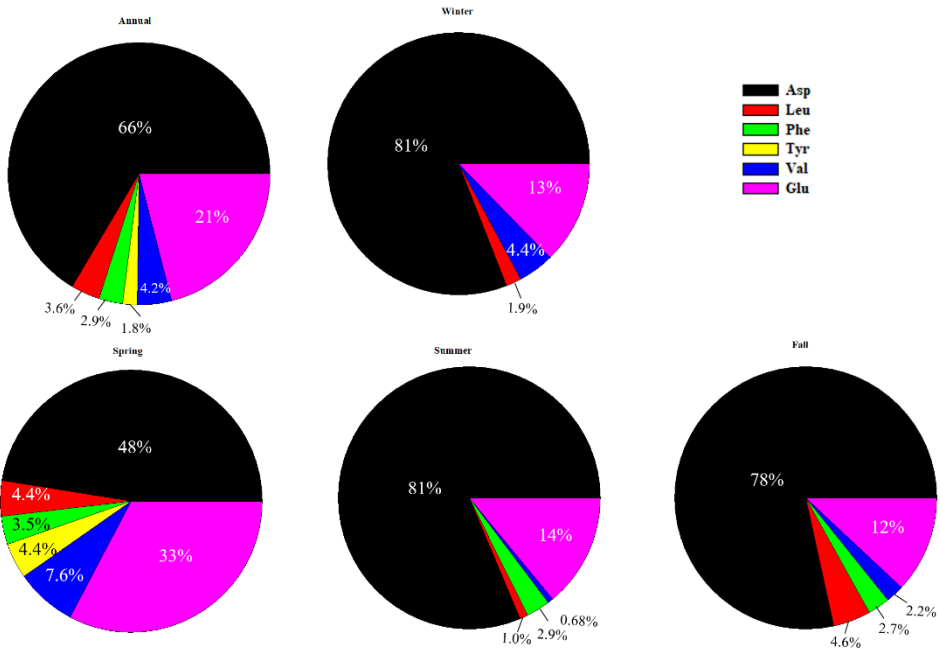


Figure 7. Seasonal variations on average mass concentration of FAAs.

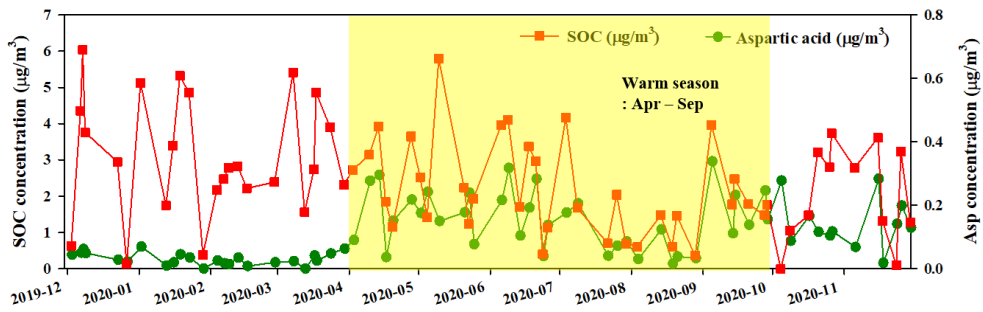


Figure 8. Time plots of SOC and Asp.

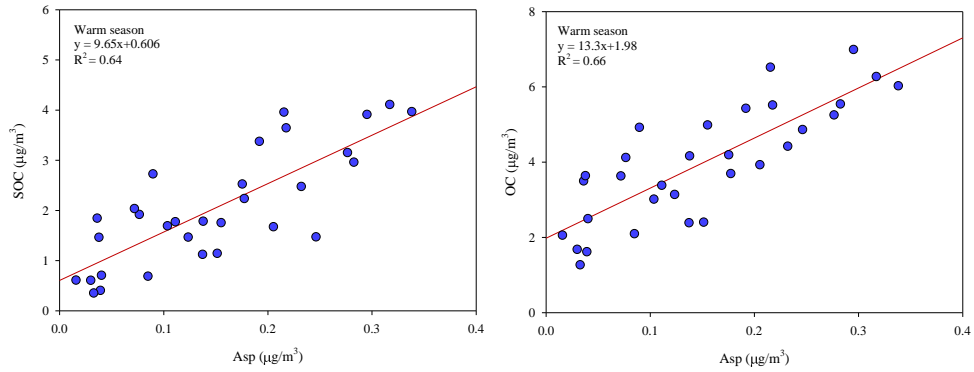


Figure 9. Scatter plots between SOC and Asp (left) and between OC and Asp (right) in warm season.

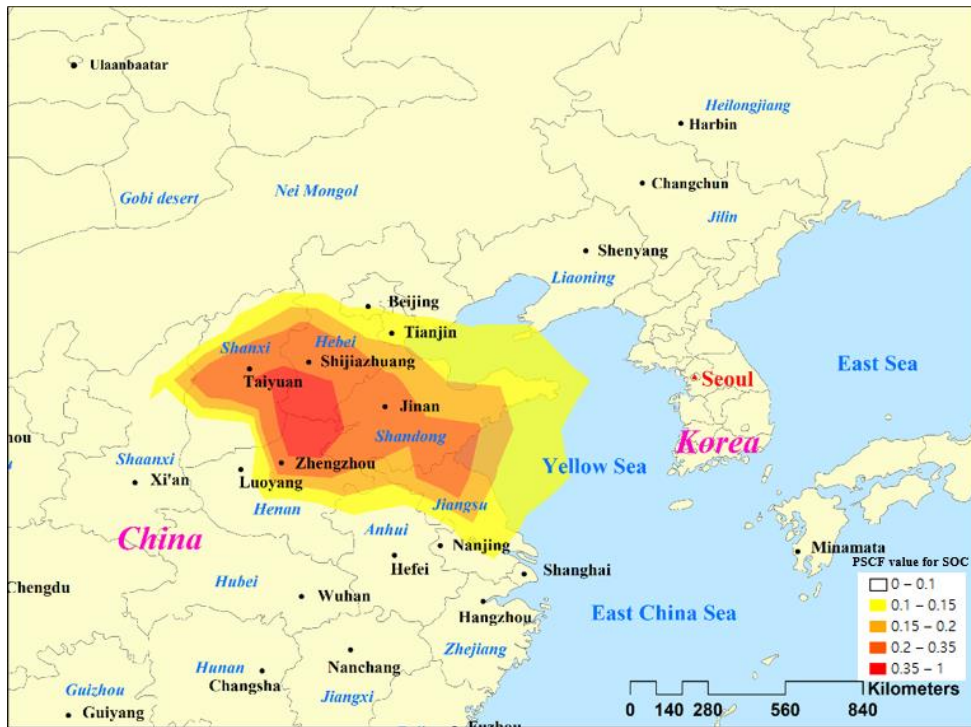


Figure 10. PSCF plot of SOC mass concentration (threshold: upper 25% of SOC mass concentration, $3.61 \mu\text{g}/\text{m}^3$)

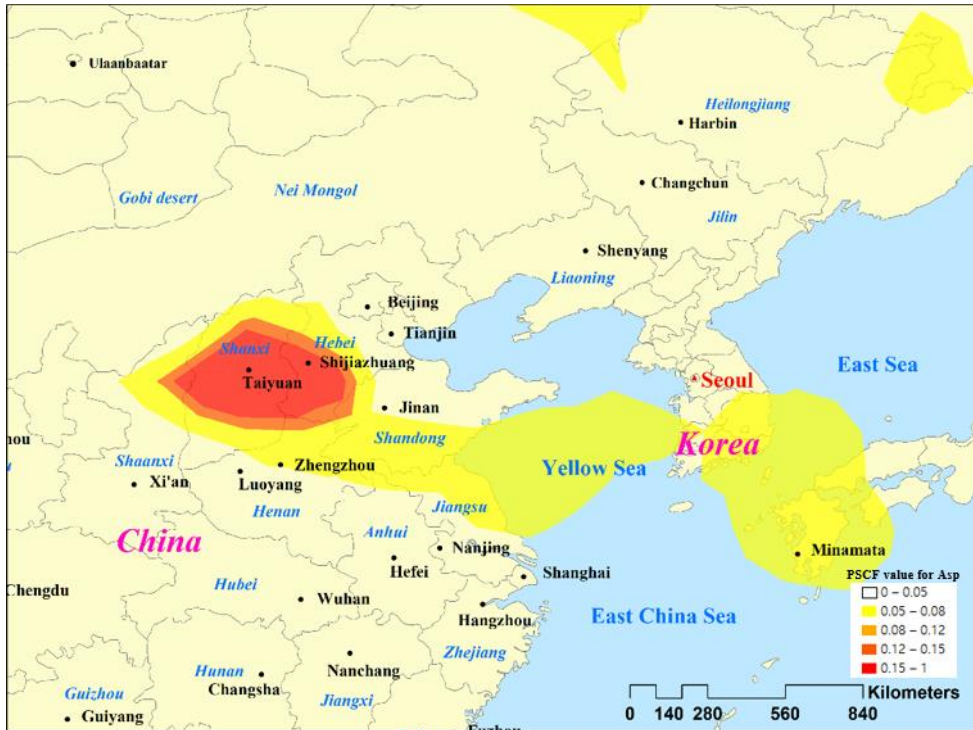


Figure 11. PSCF plot of Asp mass concentration (threshold: upper 25% of Asp mass concentration, $0.176 \mu\text{g}/\text{m}^3$).

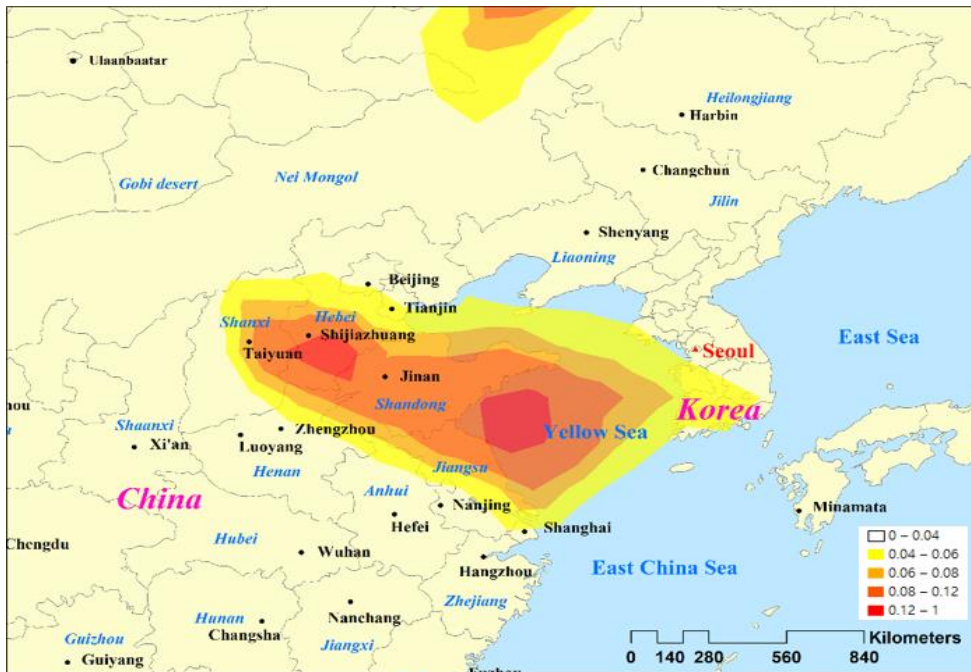


Figure 12. PSCF plot of Glu mass concentration (threshold: upper 25% of Glu mass concentration, $0.038 \mu\text{g}/\text{m}^3$).

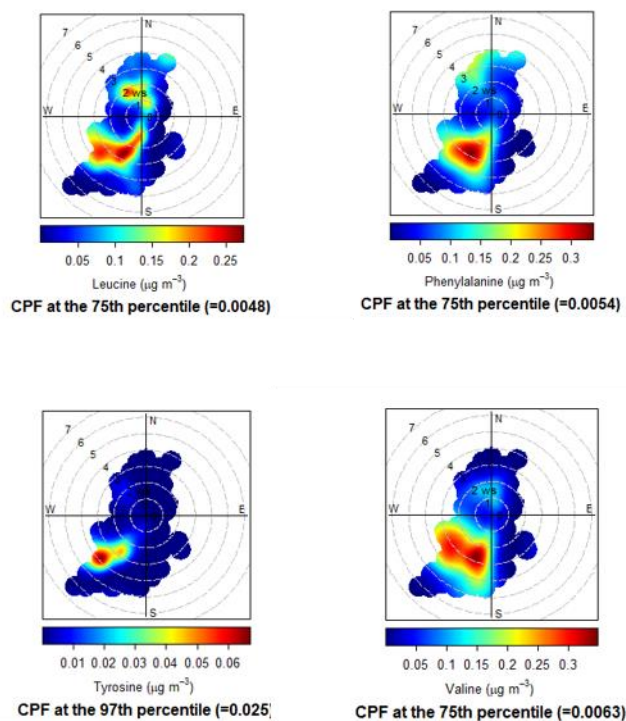


Figure 13. CPF results of Leu, Phe, Tyr, and Val.

Table 8. Factor loadings matrix after varimax rotation.

Variable	Factor 1	Factor 2	Factor 3
Val	0.968	0.123	0.04
Leu	0.959	-0.025	-0.013
Glu	0.904	0.304	-0.0202
Phe	0.899	-0.094	-0.357
Asp	0.021	0.893	-0.186
SOC	0.130	0.749	0.407
POC	-0.188	0.015	0.935

Chapter 4. Conclusions

For the selected 71 ambient PM_{2.5} samples, Chemical characteristics was investigated. The WSOC/OC ratio during the spring (0.51) and summer (0.51) were higher than those obtained in winter (0.37) and fall (0.31). When divided into cold and warm season, WSOC/OC in warm season was higher significantly than that of cold season ($p < 0.005$). Although the low concentration of SOC and WSOC were observed in summer, WSOC/OC ratio was highest in summer. The result represented that significant portion of OC can be more photo-chemically oxidized in the form of WSOC in warm season than in cold season.

The annual average concentration of total FAAs (Asp, Leu, Phe, Tyr, Val, and Glu) was 106 ± 2.81 ng/m³. Total FAAs was the highest in spring (180 ± 2.70 ng/m³), while the lowest in winter (35.0 ± 1.78 ng/m³). Asp, which was the most abundant in total FAAs, was correlated well with SOC during the warm season ($R^2 = 0.62$). Since ozone level related to hydroxyl radical formation was high in warm season, Asp could be produced by the photolysis of precursor such as asparagine (Milen and Zika, 1993). PSCF results showed the Taiyuan in the Shanxi province and Shijiazhuang in the Hebei province may be the possible source regions that affected high concentration events of SOC and Asp. The results suggested that Asp can be used as an indicator of SOA during the warm season.

The time plots of other species of FAAs (Glu, Leu, Val, Tyr, and Phe) showed the peak event in May. This peak event was probably

due to the increased release of pollen and spores in this month. CPF results suggested that the high concentration event of Leu, Val, Tyr, and Phe were commonly influenced by the southwest region where Sihwa–Banwol industrial complex is located.

The result of factor analysis is consistent with the correlation between SOC and Asp, CPF and PSCF results. The results suggested that the possible sources and source regions of FAAs in PM_{2.5} measured in Seoul: (1) SOA due to long–range transport from North China, (2) marine aerosols from Yellow Sea on the Chinese side, (3) the influence of local industry sources and, (4) airborne pollen effect in spring.

Reference

- Aggarwal, Shankar Gopala, and Kimitaka Kawamura. "Carbonaceous and inorganic composition in long-range transported aerosols over northern Japan: Implication for aging of water-soluble organic fraction." *Atmospheric Environment* 43.16 (2009): 2532–2540.
- Aznar, Margarita, Elena Canellas, and Cristina Nerín. "Quantitative determination of 22 primary aromatic amines by cation-exchange solid-phase extraction and liquid chromatography-mass spectrometry." *Journal of Chromatography A* 1216.27 (2009): 5176–5181.
- Busca, G., and C. Pistarino. "Abatement of ammonia and amines from waste gases: a summary." *Journal of Loss Prevention in the Process Industries* 16.2 (2003): 157–163.
- Chan, Man Nin, et al. "Hygroscopicity of water-soluble organic compounds in atmospheric aerosols: Amino acids and biomass burning derived organic species." *Environmental science & technology* 39.6 (2005): 1555–1562.
- Choi, Jong-kyu, et al. "Source apportionment of PM_{2.5} at the coastal area in Korea." *Science of the Total Environment* 447 (2013): 370–380.
- Chuang, Hsiao-Chi, et al. "Effects of non-protein-type amino acids of fine particulate matter on E-cadherin and inflammatory responses in mice." *Toxicology letters* 237.3 (2015): 174–180.
- Cohen, Aaron J., et al. "Estimates and 25-year trends of the global burden of disease attributable to ambient air pollution: an analysis

- of data from the Global Burden of Diseases Study 2015." *The Lancet* 389.10082 (2017): 1907–1918
- Cowie, Gregory L., and John I. Hedges. "Sources and reactivities of amino acids in a coastal marine environment." *Limnology and Oceanography* 37.4 (1992): 703–724.
- Decesari, S., et al. "Chemical features and seasonal variation of fine aerosol water-soluble organic compounds in the Po Valley, Italy." *Atmospheric Environment* 35.21 (2001): 3691–3699.
- Di Filippo, Patrizia, et al. "Free and combined amino acids in size-segregated atmospheric aerosol samples." *Atmospheric Environment* 98 (2014): 179–189.
- Dominici, Francesca, et al. "Fine particulate air pollution and hospital admission for cardiovascular and respiratory diseases." *Jama* 295.10 (2006): 1127–1134.
- Ge, X., Wexler, A. S., & Clegg, S. L. (2011). Atmospheric amines—Part I. A review. *Atmospheric Environment*, 45(3), 524–546.
- Kang, Hui, Zhouqing Xie, and Qihou Hu. "Ambient protein concentration in PM10 in Hefei, central China." *Atmospheric environment* 54 (2012): 73–79.
- Kim, Hyewon, "Characterization and source identification of PM_{2.5} organic carbon in Beijing and Seoul using organic molecular markers" . Seoul national university (2020).
- Kristensson, Adam, Thomas Rosenørn, and Merete Bilde. "Cloud droplet activation of amino acid aerosol particles." *The Journal of Physical Chemistry A* 114.1 (2010): 379–386.
- Niese, Kathryn A., et al. "The cationic amino acid transporter 2 is

- induced in inflammatory lung models and regulates lung fibrosis." *Respiratory research* 11.1 (2010): 1–9.
- Mandalakis, Manolis, et al. "Free and combined amino acids in marine background atmospheric aerosols over the Eastern Mediterranean." *Atmospheric Environment* 45.4 (2011): 1003–1009.
- Matos, João TV, Regina MBO Duarte, and Armando C. Duarte. "Challenges in the identification and characterization of free amino acids and proteinaceous compounds in atmospheric aerosols: A critical review." *TrAC Trends in Analytical Chemistry* 75 (2016): 97–107.
- Matsumoto, Kiyoshi, and Mitsuo Uematsu. "Free amino acids in marine aerosols over the western North Pacific Ocean." *Atmospheric Environment* 39.11 (2005): 2163–2170.
- McGregor, Keith G., and Cort Anastasio. "Chemistry of fog waters in California's Central Valley: 2. Photochemical transformations of amino acids and alkyl amines." *Atmospheric Environment* 35.6 (2001): 1091–1104.
- Meyers, Brian E., Dilip K. Moonka, and Robert H. Davis. "The effect of selected amino acids on gelatin–induced inflammation in adult male mice." *Inflammation* 3.3 (1979): 225–233..
- Miguel, Ann G., et al. "Allergens in paved road dust and airborne particles." *Environmental science & technology* 33.23 (1999): 4159–4168.
- Milne, Peter J., and Rod G. Zika. "Amino acid nitrogen in atmospheric aerosols: Occurrence, sources and photochemical modification."

- Journal of Atmospheric Chemistry 16.4 (1993): 361–398.
- Miyazaki, Y., et al. "Time-resolved measurements of water-soluble organic carbon in Tokyo." *Journal of Geophysical Research: Atmospheres* 111.D23 (2006).
- Mukhin, L. M., and MUKHIN LM. "THE ROLE OF VOLCANIC PROCESSES IN THE EVOLUTION OF ORGANIC COMPOUNDS ON THE PRIMITIVE EARTH." (1978).
- Murphy, S. M., et al. "Secondary aerosol formation from atmospheric reactions of aliphatic amines." *Atmospheric Chemistry and Physics* 7.9 (2007): 2313–2337.
- Park, Da-Jeong, In-Hwan Cho, and Min-Suk Bae. "Determination of Amino Acids on Wintertime PM 2.5 using HPLC–FLD." *Journal of Korean Society for Atmospheric Environment* 31.5 (2015): 482–492.
- Peters, Klaus, and Gabriele Bruckner–Schatt. "The dry deposition of gaseous and particulate nitrogen compounds to a spruce stand." *Water, Air, and Soil Pollution* 85.4 (1995): 2217–2222.
- Peterson, Jeffrey D., et al. "Glutathione levels in antigen-presenting cells modulate Th1 versus Th2 response patterns." *Proceedings of the National Academy of Sciences* 95.6 (1998): 3071–3076.
- Riva, E., et al. "PKU-related dysgammaglobulinaemia: the effect of diet therapy on IgE and allergic sensitization." *Journal of inherited metabolic disease* 17.6 (1994): 710–717.
- Saxena, Pradeep, and Lynn M. Hildemann. "Water-soluble organics in atmospheric particles: A critical review of the literature and application of thermodynamics to identify candidate compounds."

- Journal of atmospheric chemistry 24.1 (1996): 57–109.
- Scalabrin, E., et al. "Amino acids in Arctic aerosols." *Atmospheric Chemistry and Physics* 12.21 (2012): 10453–10463.
- Schade, Gunnar W., and Paul J. Crutzen. "Emission of aliphatic amines from animal husbandry and their reactions: Potential source of N₂O and HCN." *Journal of Atmospheric Chemistry* 22.3 (1995): 319–346.
- Schmeltz, Irwin, and Dietrich Hoffmann. "Nitrogen-containing compounds in tobacco and tobacco smoke." *Chemical Reviews* 77.3 (1977): 295–311.
- Seinfeld, John H., and Spyros N. Pandis. "Atmospheric Chemistry and Physics, A Wiley–Inter Science Publication." (2006).
- Shin, Ju–Young, et al. "Allergenic pollen calendar in Korea based on probability distribution models and up-to-date observations." *Allergy, asthma & immunology research* 12.2 (2020): 259.
- Silva, Philip J., et al. "Trimethylamine as precursor to secondary organic aerosol formation via nitrate radical reaction in the atmosphere." *Environmental science & technology* 42.13 (2008): 4689–4696.
- Size, Glycerol Market. "Share & Trends Analysis Report By Source (Biodiesel, Fatty Acids, Fatty Alcohols, Soap), By Type (Crude, Refined) By End Use (Food & Beverage, Pharmaceutical), By Region, And Segment Forecasts, 2020–2027, Global Glycerol Market Size, Share." *Industry Report* (2020).
- Snyder, David C., et al. "Insights into the origin of water soluble

- organic carbon in atmospheric fine particulate matter." *Aerosol Science and Technology* 43.11 (2009): 1099–1107.
- Song, Tianli, et al. "Proteins and amino acids in fine particulate matter in rural Guangzhou, Southern China: seasonal cycles, sources, and atmospheric processes." *Environmental science & technology* 51.12 (2017): 6773–6781.
- Tai, Amos PK, et al. "Meteorological modes of variability for fine particulate matter (PM_{2.5}) air quality in the United States: implications for PM 2.5 sensitivity to climate change." *Atmospheric Chemistry and Physics* 12.6 (2012): 3131–3145.
- Turpin, Barbara J., and James J. Huntzicker. "Identification of secondary organic aerosol episodes and quantitation of primary and secondary organic aerosol concentrations during SCAQS." *Atmospheric Environment* 29.23 (1995): 3527–3544.
- Verma, Vishal, et al. "Organic aerosols associated with the generation of reactive oxygen species (ROS) by water-soluble PM_{2.5}." *Environmental science & technology* 49.7 (2015): 4646–4656.
- Villena, Guillermo, et al. "Vertical gradients of HONO, NO_x and O₃ in Santiago de Chile." *Atmospheric Environment* 45.23 (2011): 3867–3873.
- Wang, Guoying, et al. "Seasonal variation characteristics of hydroxyl radical pollution and its potential formation mechanism during the daytime in Lanzhou." *Journal of Environmental Sciences* 95 (2020): 58–64.
- Wang, Xiaoyan, Renhe Zhang, and Wei Yu. "The effects of PM_{2.5} concentrations and relative humidity on atmospheric visibility in

- Beijing." *Journal of Geophysical Research: Atmospheres* 124.4 (2019): 2235–2259..
- Wedyan, Mohammed A., and Martin R. Preston. "The coupling of surface seawater organic nitrogen and the marine aerosol as inferred from enantiomer-specific amino acid analysis." *Atmospheric Environment* 42.37 (2008): 8698–8705..
- WHO, World Health Organization, Regional Office for Europe. "Health Effects of Particulate Matter: Policy Implications for Countries in Eastern Europe, Caucasus and Central Asia" (2013).
- Zhang, Qi, Cort Anastasio, and Mike Jimenez-Cruz. "Water-soluble organic nitrogen in atmospheric fine particles (PM_{2.5}) from northern California." *Journal of Geophysical Research: Atmospheres* 107.D11 (2002): AAC–3.
- Zhang, Qi, and Cort Anastasio. "Free and combined amino compounds in atmospheric fine particles (PM_{2.5}) and fog waters from Northern California." *Atmospheric Environment* 37.16 (2003): 2247–2258.

Supplementary Materials

Table S1. TOT method based on the NIOSH 5040 protocol

Step	Carrier Gas	Ramp Time (Seconds)	Temperature (°C)
OC	1 Helium (He)	60	315
	2 Helium (He)	60	475
	3 Helium (He)	60	615
	4 Helium (He)	90	870
	Helium (He)	Oven heaters are turned off to cool down the oven	
EC	5 2% O ₂ in He	45	550
	6 2% O ₂ in He	45	625
	7 2% O ₂ in He	45	700
	8 2% O ₂ in He	45	775
	9 2% O ₂ in He	45	850
	10 2% O ₂ in He	120	910
Cal gas (CH ₄) + He/Ox		External Std. Calibration and cool down	

Table S2. MS parameters for FAAs analysis

MS parameters	
Collision Gas (CAD)	7
Curtain Gas (CUR)	20
Ion source Gas 1 (GS1)	45
Ion source Gas 2 (GS2)	50
IonSpray Voltage (IS)	3500
Temperature (TEM)	300
Interface Heater (ihe)	ON

Table S3. Multiple reaction monitoring (MRM) transition

	Compounds	Q1 Mass (Da)	Q3 Mass (Da)	DP (volts)	EP (volts)	CE (volts)	CXP (volts)
Asp	Quantitation ion	134.006	88.2	41	10	15	6
	Qualifier ion	134.006	74.1	50	10	19	4
Cys	Quantitation ion	241.078	152	36	10	19	12
	Qualifier ion	241.078	120	36	10	25	10
Leu	Quantitation ion	132.102	86.1	41	10	13	6
	Qualifier ion	132.102	44.2	41	10	31	6
Met	Quantitation ion	150.114	104.1	31	10	13	8
	Qualifier ion	150.114	133.1	45	10	11	12
Phe	Quantitation ion	166.153	120.1	41	10	17	22
	Qualifier ion	166.153	103.1	41	10	37	8
Tyr	Quantitation ion	182.185	165.1	36	10	13	14
	Qualifier ion	182.185	136.1	36	10	17	12
Val	Quantitation ion	118.113	72.2	36	10	15	6
	Qualifier ion	118.113	55.1	36	10	27	6
Glu	Quantitation ion	147.952	84.1	41	10	21	6
	Qualifier ion	147.952	102.1	41	10	15	6
Ser	Quantitation ion	105.808	60.2	31	10	15	2
	Qualifier ion	105.808	88.1	31	10	13	6
IS	IS	167.999	122.1	26	10	17	8

Table S4. HPLC gradient steps

Time (min)	% Eluent B
0	5
2	5
3	10
4	90
6	90
6.5	5
10	5

Table S5. Retention time, LOD, and LOQ of FAAs

Compounds	Retention time (min)	LOD (nM)	LOQ (nM)
Asp	1.29	7.5	18.8
Cys	1.27	4.2	10.4
Leu	1.93	3.8	7.6
Met	1.83	6.7	16.8
Phe	3.83	3.0	15.1
Tyr	2.05	5.5	27.6
Val	1.53	8.5	21.3
Glu	1.30	4.3	8.5
Ser	1.27	23.8	47.6

Table S6. Recovery result for FAAs

Compounds	Formula	Calibration curve (R ²)	Recovery (%) (n=5)
			Mean (RSD, %)
Aspartic acid (Asp)	C ₄ H ₇ NO ₄	0.9958	72 (2.7)
Cystine (Cys)	C ₆ H ₁₂ N ₂ O ₄ S ₂	0.9996	77 (6.3)
Leucine (Leu)	C ₆ H ₁₃ NO ₂	0.9997	105 (3.7)
Methionine (Met)	C ₅ H ₁₁ O ₂ NS	0.9998	91 (3.3)
Phenylalanine (Phe)	C ₉ H ₁₁ NO ₂	0.9991	107 (2.5)
Tyrosine (Tyr)	C ₉ H ₁₁ NO ₃	0.9988	114 (0.86)
Valine (Val)	C ₅ H ₁₁ NO ₂	0.9998	70 (1.6)
Glutamic acid (Glu)	C ₅ H ₉ NO ₄	0.9992	76 (4.2)
Serine (Ser)	C ₃ H ₇ NO ₃	0.9994	87 (3.1)

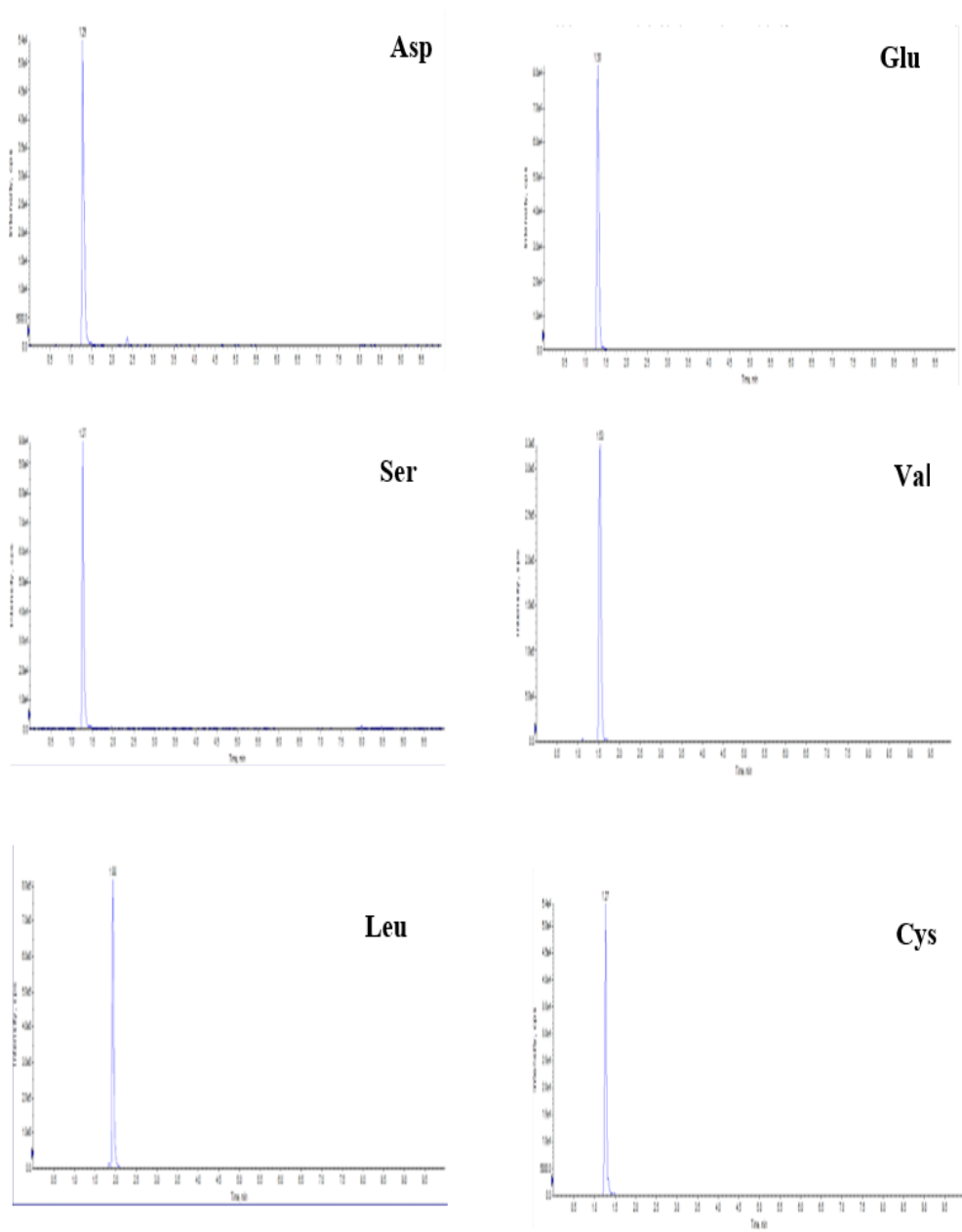


Figure S1. Chromatogram from a standard mixture.

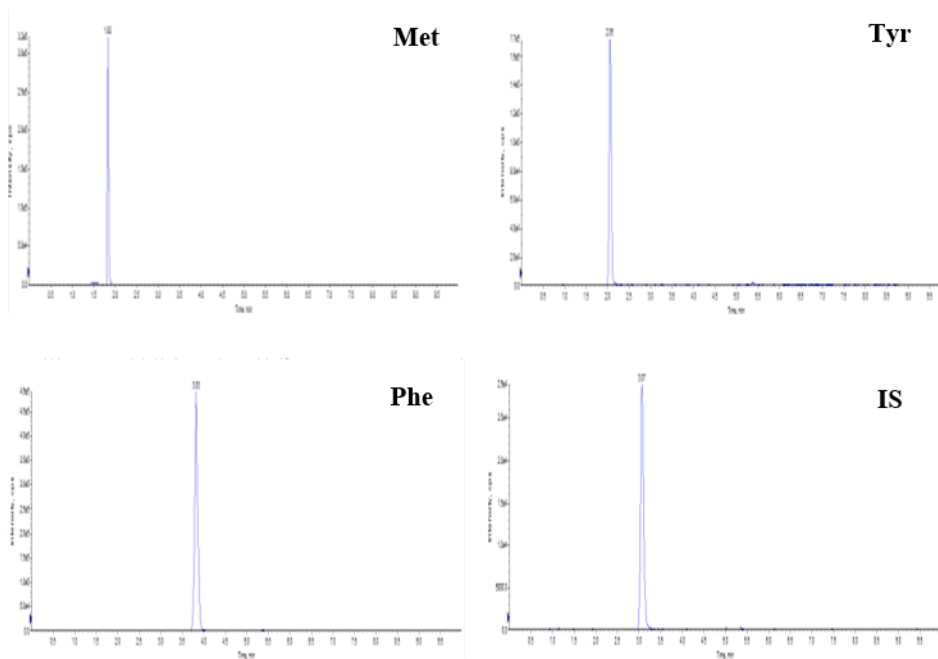


Figure S2. Chromatogram from a standard mixture (Continued).

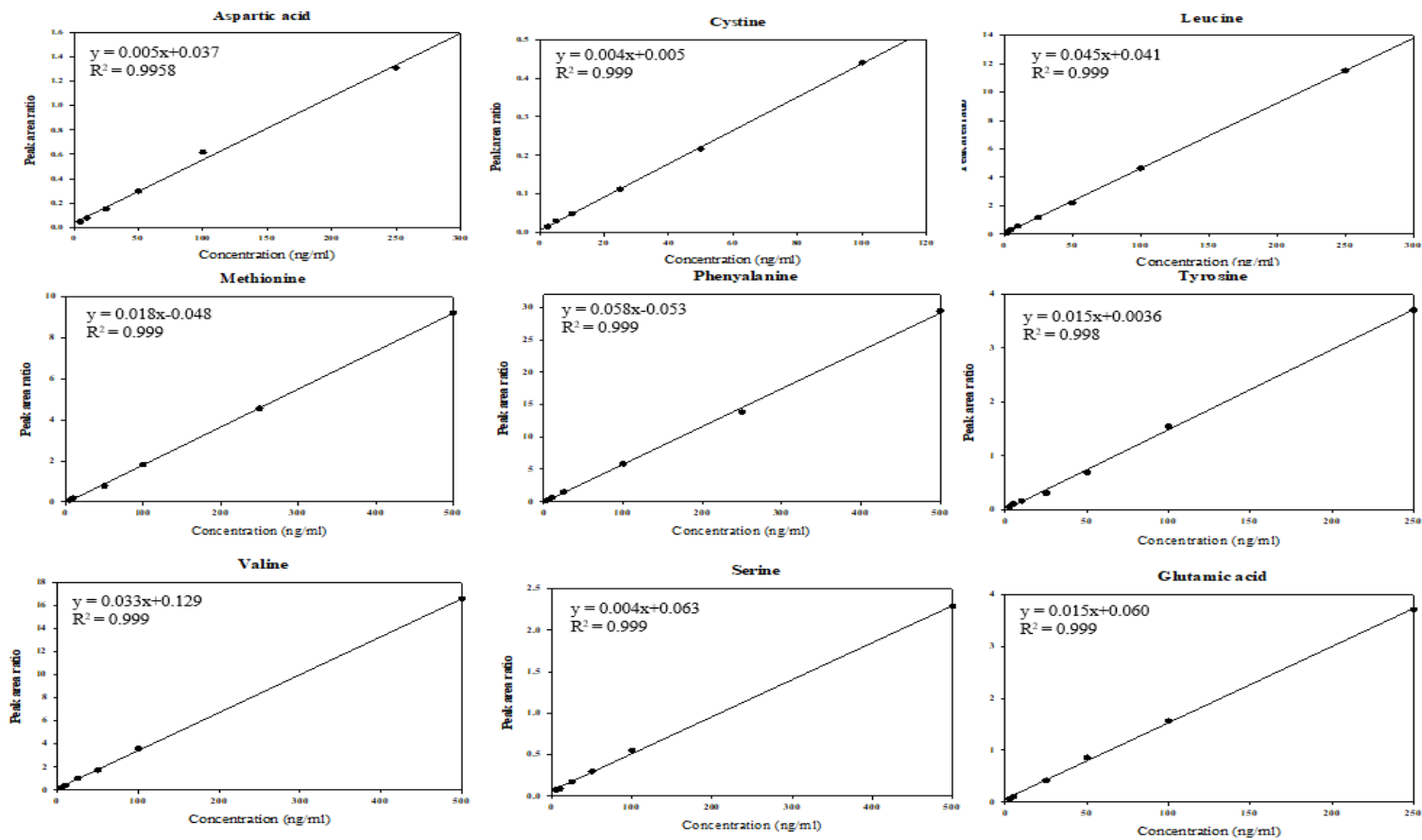


Figure S3. Calibration curve of individual FAA.

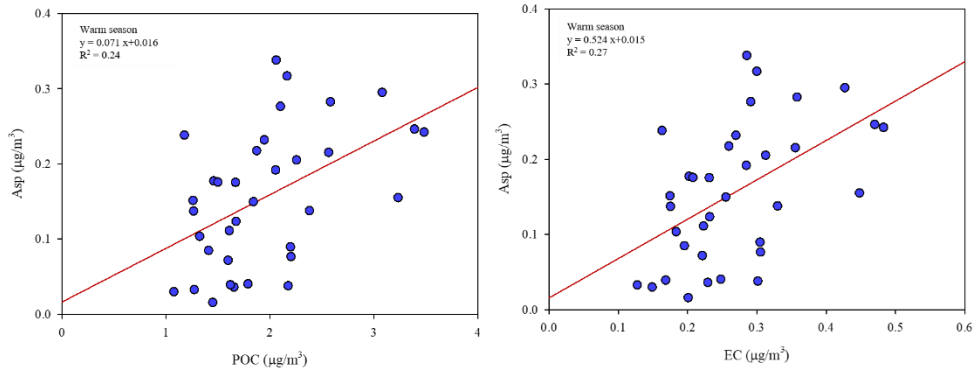


Figure S4. Scatter plots between POC and Asp (left) and between EC and Asp (right) in warm season.

Table S7. Summary of PM_{2.5} species concentration during the study period

Species	Cold season (Dec 2019–Mar 2020, Oct –Nov 2020)	Warm season (Apr–Sep 2020)
PM _{2.5} ($\mu\text{g}/\text{m}^3$)	28.7 ± 1.89	20.7 ± 1.55
OC ($\mu\text{g}/\text{m}^3$)	5.38 ± 1.49	3.76 ± 1.58
EC ($\mu\text{g}/\text{m}^3$)	0.39 ± 1.49	0.25 ± 1.40
POC ($\mu\text{g}/\text{m}^3$)	2.83 ± 1.49	1.83 ± 1.39
SOC ($\mu\text{g}/\text{m}^3$)	2.15 ± 2.58	1.78 ± 2.00
WSOC ($\mu\text{g}/\text{m}^3$)	2.03 ± 1.80	1.77 ± 1.82
NO ₃ ⁻ ($\mu\text{g}/\text{m}^3$)	7.43 ± 2.67	2.00 ± 3.65
SO ₄ ⁻ ($\mu\text{g}/\text{m}^3$)	3.65 ± 1.94	4.31 ± 1.76
NH ₄ ⁺ ($\mu\text{g}/\text{m}^3$)	3.51 ± 2.31	2.41 ± 1.92
Σ crustal elements ($\mu\text{g}/\text{m}^3$)	1.84 ± 1.71	1.41 ± 1.89
Σ non–crustal element ($\mu\text{g}/\text{m}^3$)	0.57 ± 1.86	0.19 ± 2.37
FAA (ng/m ³)		
Asp	47.6 ± 2.54	122 ± 2.22
Leu	4.67 ± 2.42	5.36 ± 2.68
Phe	5.14 ± 1.60	5.89 ± 1.89
Tyr	N.D.	58.2 ± 2.26
Val	6.21 ± 1.66	11.2 ± 3.11
Glu	13.3 ± 2.31	28.0 ± 3.58
Total FAAs	65.1 ± 2.53	175 ± 2.45

국문 초록

서울시 초미세먼지 내 유리 아미노산 농도 특성 파악 연구

이미래

서울대학교 보건대학원

환경보건학과

초미세먼지 내 수용성 유기탄소(Water-soluble organic carbon, WSOC)는 다른 성분들과 비교하여 물에 잘 녹기 때문에, 폐액에 흡수되어 호흡기 질환을 일으켜 인체에 유해한 영향을 미칠 수 있다. 이러한 WSOC 중 질소를 포함하는 성분인 아미노산은 염기성인 아미노기와 산성인 카르복시기를 가지고 있어서 대기 중의 완충작용 및 산도에 영향을 미친다. PM_{2.5}에 존재하는 아미노산 성분의 건강 영향에 대한 연구 사례는 현재까지 많이 수행되지 않았으나, 알레르기 염증 반응과 관련이 있는 것으로 보고되었다. 또한, 아미노산 흡입으로 인하여 폐 내 아미노산 조성의 변이가 발생하면, 면역 반응에 악영향을 미칠 가능성이 있다고 보고되었다. 따라서 PM_{2.5} 내 존재하는 아미노산 성분의 발생 원인과 인체 유해성을 정확히 규명하기 위해서 해당 성분의 조성과 농도 수준을 파악하는 것은 매우 중요하다. 본 연구는

서울대학교 보건대학원 옥상에서 고용량 공기 채취기를 이용하여 포집된 시료를 분석에 이용하였다. 또한, 별도의 유도체화 과정이 필요하지 않고, 낮은 농도의 정량 한계 분석이 가능한 액체크로마토그래피 질량분석기(LC-MS/MS)를 이용하여 PM_{2.5} 내 존재하는 유리 아미노산 성분의 정성 및 정량법을 연구하였다.

본 연구 결과, SOA를 추정하는 지표로 사용되는 WSOC/OC는 warm season (4월-9월)에 cold season보다 유의하게 높은 것으로 나타났다 (Mann-Whitney 순위 합 검정 수행 시 $p < 0.005$). 또한 WSOC는 POC ($R^2 = 0.16$)보다 SOC ($R^2 = 0.60$)와 상관성이 높은 것으로 나타났다. 이러한 결과는 OC의 상당 부분이 광화학적 노화 과정을 거쳐 WSOC 성분으로 존재하는 것으로 사료된다. WSOC의 성분 중 질소를 포함하는 성분인 유리 아미노산 성분 중 Aspartic acid는 warm season에 SOC와 높은 상관성($R^2 = 0.64$)이 확인되어, SOA 생성과 관련이 있는 것으로 나타났다. SOC와 Aspartic acid 그리고 대기 중 반응성이 낮은 것으로 알려진 Glutamic acid의 장거리 이동 영향을 확인하기 위하여 PSCF 모델링을 수행하였다. 그 결과 공통적으로 중국 화북지역의 주요 복합 산업단지가 조성된 타이위안과 스좌장 지역이 주요 오염원으로 분석되었다. 추가적으로 Glutamic acid의 경우, 중국쪽 황해 지역의 영향을 받는 것으로 분석되었다. Glutamic acid, Leucine, Phenylalanine, Tyrosine, Valine 성분은 공통적으로 5월에 급격하게 증가하는 피크 사례가 확인되었으며 이는 봄철에 기승하는 꽃가루의 영향으로 추정된다. 꽃가루 영향 외에 해당 유리 아미노산 성분들의 잠재적인 오염원을 추정하기 위하여, CPF 수행한 결과, 공통적으로 샘플링 사이트 기준으로 시화-반월공단이 위치한 남서쪽 지역의 영향을 받는 것으로 나타났다. 이러한 본 연구 결과에 따르면, PM_{2.5} 내 유리 아미노산 성분은 (1)중국 화북지역으로부터의 장거리 이동에 따른 이차

생성 에어로졸의 영향, (2)식물 플랑크톤과 같은 해양 기원 오염원, (3)국지적 산업 오염원의 영향, (4)봄철 꽃가루의 영향을 받는 것으로 추정된다.

주요 단어 : 초미세먼지, 수용성 유기탄소, 유리 아미노산, 이차생성 에어로졸, 액체크로마토그래피-질량분석기

학번 : 2019-22005